Microfluid Nanofluid (2012) 12:221–228
DOI 10.1007/s10404-011-0866-6

RESEARCH PAPER

Optothermal sample preconcentration and manipulation with temperature gradient focusing

M. Akbari · M. Bahrami · D. Sinton

Received: 1 June 2011 / Accepted: 30 July 2011 / Published online: 12 August 2011

Abstract In this article, we present an optothermal analyte preconcentration method based on temperature gradient focusing. This approach offers a flexible, noninvasive technique for focusing and transporting charged analytes in microfluidics using light energy. The method uses the optical field control provided by a digital projector as established for particle manipulation, to achieve analogous functionality for molecular analytes for the first time. The optothermal heating system is characterized and the ability to control of the heated zone location, size, and power is demonstrated. The method is applied to concentrate a sample model analyte, along a microcapillary, resulting in almost 500-fold local concentration increase in 15 min. Optically controlled upstream and downstream transport of a focused analyte band is demonstrated with a heater velocity of $\sim$170 μm/min.

Keywords Optothermal · Temperature gradient focusing · Preconcentration · Analyte manipulation · Microfluidics

Electronic supplementary material The online version of this article (doi:10.1007/s10404-011-0866-6) contains supplementary material, which is available to authorized users.

M. Akbari · M. Bahrami
Mechatronic Systems Engineering, Simon Fraser University, 250-13450 102 Avenue, Surrey, BC V3T 0A3, Canada

D. Sinton (✉)
Department of Mechanical and Industrial Engineering, University of Toronto, 5 King's College Rd., Toronto, ON M5S 3G8, Canada
e-mail: sinton@mie.utoronto.ca

1 Introduction

Widespread application of point-of-care (POC) medical diagnostic systems will require operation with relatively small volumes of highly complex fluids (Yager et al. 2006, 2008 ; Dupuy et al. 2005; Toner and Irimia 2005; Myers and Lee 2009). Challenges in the development of these systems include the detection of very dilute solutions of analytes in small volumes, the mismatch between small volumes employed in the analysis, and larger volumes required to facilitate testing, and the need to transport the sample and/or the test result. To address some of these challenges, several microfluidics-based methods for analyte preconcentration and manipulation have been developed (Ross and Locascio 2002), examples include field amplified stacking (FAS) (Mikkers et al. 1979; Burgi and Chien 1991; Chien and Burgi 1992; Albert et al. 1997), isotachophoresis (ITP) (Boček et al. 1978; Everaerts et al. 1979), sweeping (Quirino and Terabe 1998, 1999; Isoo and Terabe 2003), electric field gradient focusing (EFGF) (Koegler and Ivory 1996; Tolley et al. 2002; Astroga-Wells et al. 2005), and temperature gradient focusing (TGF) (Ross and Locascio 2002, Balss et al. 2004; Hoebel et al. 2006; Huber and Santiago 2007; Kamande et al. 2007; Munson et al. 2007; Shackman and Ross 2007; Sommer et al. 2007; Matsui et al. 2007; Tang and Yang 2008; Becker et al. 2009; Ge et al. 2010).

In TGF, the charged analytes are concentrated locally by balancing the bulk flow in a channel against the electrophoretic migrative flux of an analyte along a controlled temperature profile (Ross and Locascio 2002). The principle behind the TGF mechanism is illustrated in Fig. 1. The temperature gradient is critical as local focusing of analytes occurs only at the point in the channel where the analyte velocity due to bulk flow cancels that due to electrophoresis, which is temperature dependent (Ross and Locascio 2002).

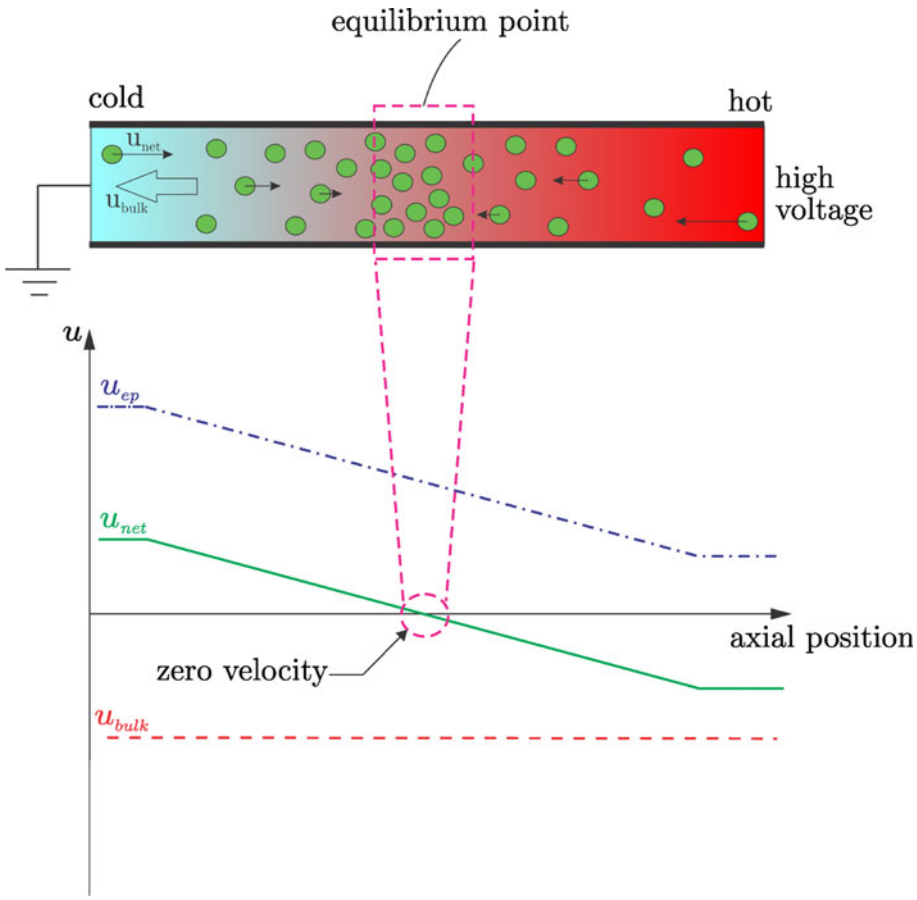

Fig. 1 Schematic illustration of temperature gradient focusing in a straight microchannel. A linear temperature gradient is produced with hot and cold regions on the right and left, respectively. By applying a high voltage, charged particles (depicted by *circles*) move away from the ground electrode (to the right) with the electrophoretic velocity of u_{ep}, while the bulk velocity is in the opposite direction. The electrophoretic velocity varies along the temperature gradient and is balanced by the constant bulk velocity at an equilibrium point, where the net velocity becomes zero

Available methods that can provide the required temperature variations include thin-film heating elements made of platinum (Pt), indium tin oxide (ITO), and non-metallic polysilicon (Yang et al. 2004; Kaigala et al. 2008; Liao et al. 2005); heating/cooling blocks (Ross and Locascio 2002; Balss et al. 2004; Sommer et al. 2007); embedded resistive wires or silver-filled epoxy (Fu et al. 2006; Vigolo et al. 2010); external Peltier modules (Ross and Locascio 2002; Huber and Santiago 2007; Liu et al. 2002); localized convective heating (Lee et al. 2004, Wang et al. 2003); infrared, visible, or microwave radiation (Duhr and Braun 2006; Krishnan et al. 2009; Oda et al. 1998; Ke et al. 2004; Issadore et al. 2009); chemical reactions (Guijt et al. 2003); and Joule heating (Sommer et al. 2007; Erickson et al. 2003). Among the abovementioned methods, heating/cooling blocks (Ross and Locascio 2002; Balss et al. 2004; Sommer et al. 2007), Peltier elements (Huber and Santiago 2007; Matsui et al. 2007), and Joule heating in a variable cross-section microchannel (Ross and Locascio 2002; Sommer et al. 2007) have been used for analyte preconcentration with TGF.

Optical methods have been widely applied to manipulate particles (Grier 2003; Chiou et al. 2005, 2008; Kumar et al. 2010; Yang et al. 2009) and bulk fluids (Terray et al. 2002; Liu et al. 2005; Krishnan et al. 2009) in microfluidics, predominantly under the name of optofluidics (Psaltis et al. 2006). Digital projection systems and digital micromirror arrays offer excellent spatial control of lighting relatively inexpensive, commercially available components. Most notably, a projected image on a photoconductive surface enabled the dynamic reconfiguration of planar electrodes that enabled the control of planar particle motion in arbitrary manner (Chiou et al. 2005). A similar method was applied to control flow, and ultimately the microfluidic structure, using a temperature-dependent viscosity fluid and local optothermal heating (Krishnan and Erickson 2011). The flexibility offered by digital projection optics has thus been applied using various strategies for particle and bulk fluid manipulation, however, an analogous method has not been developed to date for charged molecules, the most common analytes of interest in micro total analysis systems (Arora et al. 2010).

In the present study, an optothermal analyte preconcentration and manipulation method is developed using a commercial video projector and beam shaping optics. The major advantage associated with this method is its flexibility, which enables on-demand control of the location, size, and the amount of heat energy delivered. This enables the dynamic control of the focused band location and its on-demand transportation to, for instance, a sensor. Moreover, since the

proposed method is noninvasive, predefined geometries and/or complex fabrication methods associated with integrated heaters are avoided, leading to a much simpler system. Since lower applied electric fields can be used for preconcentration, the instabilities of Joule heating effect-based systems are also avoided. Most importantly, these results demonstrate a non-invasive way to concentrate and manipulate charged analytes in microfluidics, independent of fluid flow. This capability could enable a variety of analysis protocols not possible where flow and diffusion are the only modes of transport. We assessed the thermal characteristics of the optothermal approach using a temperature-dependent fluorescent dye. The optothermal approach is applied to preconcentrate charged analytes using TGF, and optically manipulate analytes independent of fluid flow.

2 Experimental section

2.1 Experimental setup

An inverted epi-fluorescent microscope (Jenco, Oregon) equipped with a 5×, 0.12 N.A. long distance objective, rhodamine B (excitation: band pass 546 nm, emission: band pass 600 nm) and green (excitation: band pass 540 nm, emission: band pass 580 nm) filter sets, a broadband mercury illumination source, and a digital CCD camera were used. Image acquisition and storage were controlled by Zarbco video toolbox (Ver.1.65) software. Ultra-small pressure driven flow was produced using hydrostatic pressure (i.e., adjusting the relative heights of two external reservoirs). A commercial video projector (Sony, 3-LDC BrightEra, 190 W Mercury lamp, 1600/2000 ANSI lumens) equipped with special optics was used for optothermic control of the system. Figure 2 illustrates the experimental setup, which was designed to control the local fluid temperature in the capillary. The location, size, and amount of heat that entered the heated area were controlled by adjusting the heater image from an external computer.

2.2 Materials and microfluidic assembly

Background electrolyte of Tris-Borate buffer (900 mM, pH = 8.5) was used for all experiments. Laser grade temperature sensitive dye, rhodamine B (Sigma Aldrish, St. Louis, MO), was used for temperature measurements. Fluorescein was purchased from Invitrogen (Invitrogen Inc., ON) for focusing demonstrations.

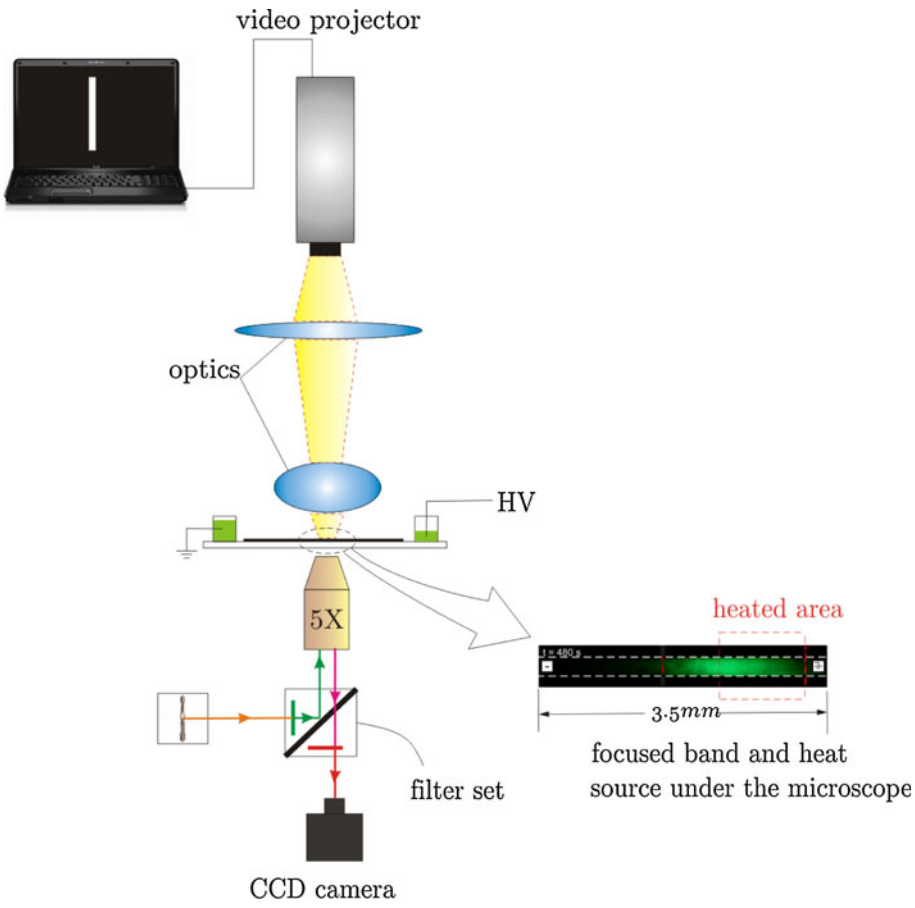

Fig. 2 Schematic of the experimental setup designed to optically control the local fluid temperature. The heater image is projected onto the surface of the microchannel providing a heated area with adjustable width. The temperature profile is used to increase the local concentration of sample analytes. Pressure control is accomplished by adjusting the relative heights of two external reservoirs. High voltage power supply is used to provide the appropriate electromigrative velocities

A 50-mm-long rectangular borosilicate glass capillary (Vitrocom, NJ) with nominal inner dimensions of 20 μm × 200 μm was used as the microchannel. The capillary was mounted on a Plexiglas substrate (25 mm × 75 mm × 1 mm) using an acrylic double sided tape (Adhesives Research, Inc.). The substrate was cut to the size using a CO_2 laser system (Universal Laser System, Model VSL 3.60, Scottsdale, AZ). Pipette tips were cut, inverted (wide side down), and epoxied at the channel ends to interface to the external fluidics. A black electric tape was fixed on the surface of the microchannel, serving as a light absorbing material. Images were projected onto the surface of the black surface using the optical setup explained in Sect. 2.1.

2.3 Temperature measurement

We performed in situ temperature field imaging based upon the temperature-dependent quantum efficiency of rhodamine B dye, using the method described in Refs. (Erickson et al. 2003; Ross et al. 2001). In brief, 0.3 mM rhodamine B in 900 mM Tris-borate buffer solution was prepared and introduced into the microchannel. A background and an isothermal "cold field" intensity image of the system were taken before each experiment. Following the acquisition of the cold field image, a rectangular strip of light was projected on the surface of the black tape to provide localized heating. Images were taken every 2 s with a resolution of 1280 × 1024 pixels, spanning a length of 3.5 mm of the channel. To extract the in-channel temperature profiles, the background image was first subtracted from each raw image and the cold field. The corrected raw images were then normalized with the corrected cold field images. The intensity values of the treated images were then converted to temperature using the intensity versus temperature calibration described as follows: a Plexiglas reservoir containing approximately 0.1 ml rhodamine B dye (0.3 mM in 900 mM Tris-Borate buffer) was fabricated using a laser system (Universal laser Microsystems Inc., USA) with an embedded k-type thermocouple. The voltage read by the thermocouple was then recorded by Labview 8.5 software (National Instruments, USA) via a standard data acquisition card (National Instruments, 16-bit, 250 KS/s). Initially the reservoir was loaded with dye solution at room temperature and the entire system was heated to approximately 75°C. The system was allowed to cool in air while intensity images were taken at specified intervals and the data acquisition system recorded the instantaneous thermocouple readings. A low-pass filter was employed to cut off the high frequency noises in the thermocouple readings. Random locations close to the thermocouple in the calibration images were then selected and their average intensity at each temperature was normalized such that an intensity of 1 corresponded to the temperature of 26°C. The calibration curve agreed well with the results reported in previous works (Guijt et al. 2003; Erickson et al. 2003; Ross et al. 2001). A more detailed description of the calibration process is provided in the Supplementary Material. It should be noted that since the channel depth in this study is much smaller than its width, the monitored 2D fluorescence intensity accurately represents the temperature field of the fluid within the microchannel.

2.4 Focusing protocol

Focusing experiments were performed using 0.1 mM of fluorescein in 900 mM Tris-Borate buffer at the pH of 8.5. Before each experiment, the channel and reservoirs were flushed with distilled water and buffer for at least 15 min. Both reservoirs were emptied, and 0.1 mM fluorescein solution was introduced in one reservoir and the channel was allowed to fill with the hydrostatic pressure. Then, the other reservoir was filled with fluorescein and the pressure head was applied. The heat source was projected on the surface of the black tape, the electric field was switched on after the steady state temperature was achieved, and image acquisition was performed every 20 s. After the electric potential was applied to the channel, the pressure head was adjusted until the focused band was observed.

3 Results and discussion

Figure 3 demonstrates the ability of the proposed optothermal approach to provide localized heating and control the location of the heated area by adjusting the projected image. These results demonstrate localized heating through the proposed optothermal strategy, and indicate that the temperature profile along the channel due to the localized heating has a Gaussian distribution as is expected from axial conduction heat transfer. As shown, a temperature increase up to 20°C (maximum temperature achieved in this experiment was about 50°C) was obtained for a heater with the width of 1.5 mm. Owing to the low Peclet number in our experiments ($\sim$0.015 for the velocities on the order of 0.2 mm/s), convective heat transfer and flow effects tend to have negligible influence on the temperature distribution.

The thermal response of the heating system is shown in Fig. 4. The maximum temperature along the channel is reported for each data point. After the heater image is projected, the temperature rises quite quickly but the rate slows with time and reaches its steady-state condition after about 25 s. The heating and cooling rates measured in this study are $\sim$0.8°C/s for a typical heater width of 1.5 mm. Note that the heating and cooling rates vary with the heat source width such that a smaller heater size leads to faster heating/cooling ramps. Our measurements also showed that

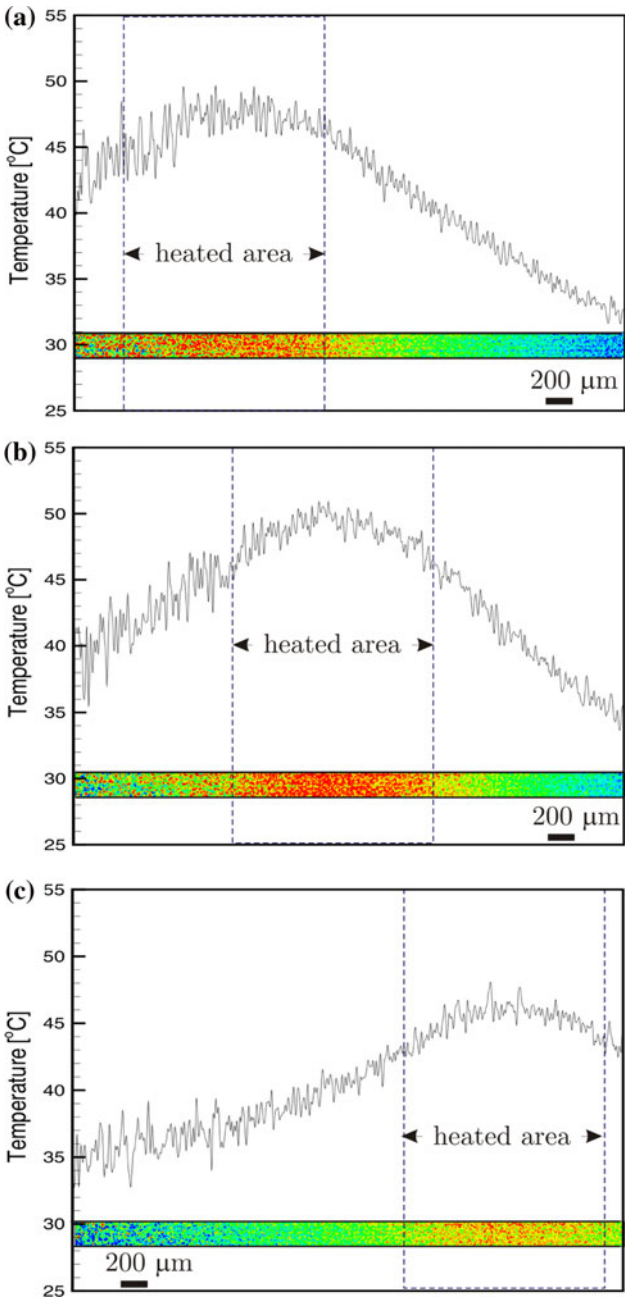

Fig. 3 Demonstration of heater location control and the resulting temperature field. The microchannel was heated at three different locations **a** left edge, **b** middle, and **c** right edge with the heater width of approximately 1.5 mm. The heater location was controlled by an external computer. Images were taken for the no flow condition and processed with the method described in Sect. 2.1. The total field of view for each image was 3.5 mm. *Dashed rectangles* indicate the location of the heated area. The temperature profile along the channel was obtained by taking the cross-sectional averaging at each axial location

the maximum temperature varies almost linearly with the width of the projected heater. This is expected as more heat is transferred to the fluid inside the microchannel for larger heat sources.

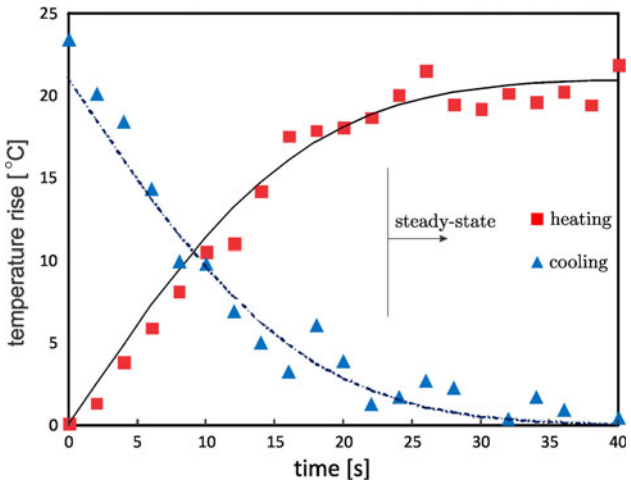

Fig. 4 Variation of maximum temperature, $T - T_{\text{room}}$, versus time for a heater width of approximately 1.5 mm. *Symbols* represent the experimental data and the *lines* represent fitted curves. Each data point was obtained by finding the maximum temperature along the microchannel. Temperature at each axial location was obtained by taking the cross-sectional average

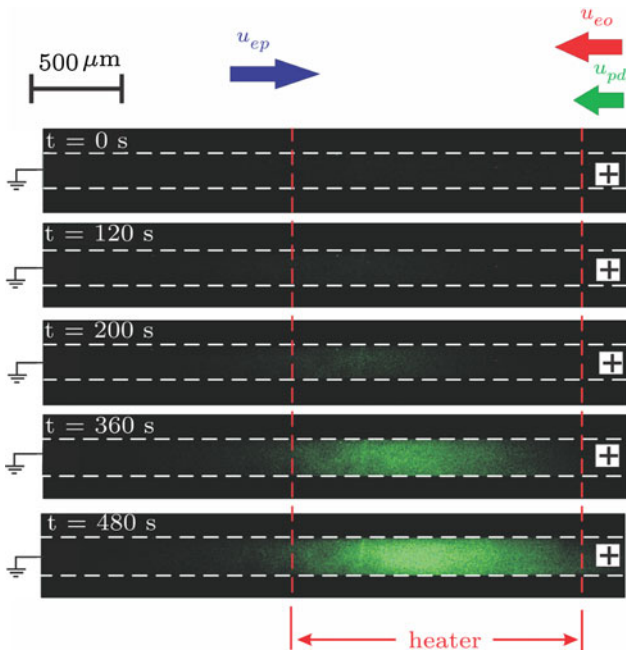

Fig. 5 Image sequence of fluorescein focusing using the optothermal heating method. The applied electric field is 200 V/cm with positive polarity on the right and ground on the left. Pressure driven velocity (resulting from 25-mm-H_2O hydrostatic head) is in favor of the electroosmotic flow from right to left. The electrophoretic velocity of fluorescein is from left to right

The ability to locally concentrate a model analyte, fluorescein dye, was achieved by combining the optothermal heating strategy with the temperature gradient focusing approach. Figure 5 shows the image sequences of the focusing experiment. The applied electric field for this experiment was 200 V/cm with the positive polarity on the

right reservoir. The projected heater was 1.5-mm wide. Fluorescein molecules migrate from left to right due to their negatively charged surface, while the electroosmotic velocity is from right to left. To balance the net velocity of the fluorescein molecules, a 25-mm-H_2O pressure head, which was accomplished by adjusting the relative heights of two external reservoirs, was applied in favor of the electroosmotic flow (i.e., from right to left). Note that the symmetric shape of the temperature profile yields two possible locations for focusing (i.e., where $u_{net} = 0$). However, focusing only occurs at one of these points, where $du_{net}/dx < 0$ and species depletion occurs at the other one. The current was monitored during the experiment to ensure that the Joule heating effect did not disturb the focused band. No change in the measured current versus time was observed throughout the entire experiment, which suggests that Joule heating effect was negligible.

Variation of normalized peak concentration versus time for two trials is plotted in Fig. 6. Normalized peak concentration was calculated as the ratio of maximum fluorescence intensity at each time over the maximum initial intensity of the dye. The experiment was run twice to ensure the reproducibility of the results. After approximately 15 min of focusing, a 500-fold concentration enrichment was achieved with an almost linear increase over time. This trend is consistent with the results obtained by Ross and Locascio (2002). Stability of the focused band was examined by monitoring the concentration peak location over time. No change in the location of the peak concentration was observed within the period of 15 min.

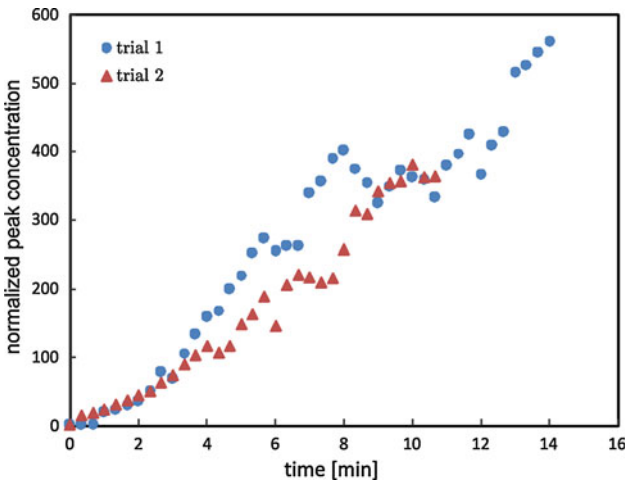

Fig. 6 Peak sample concentration versus time for two different focusing trials. The normalized concentration was calculated from the measured maximum fluorescence intensity at each time over the initial intensity. Almost 500-fold enrichment was obtained within 15 min

A key benefit of optical control in microfluidics is the flexibility it provides. On-demand transport and manipulation of the focused band of analyte was achieved here by moving the projected heater image using the external computer. Figure 7 shows the image sequences of the model analyte, fluorescein, band transported in two directions, as well as the heater location at each step. The direction and magnitude of the pressure driven flow and electric field remained unchanged from those applied in Fig. 4. Movies showing the controlled translation of the analyte band are available in Supplementary Material. To ensure that the focused band is transported only by moving the heater image, the stability of the focused band at the initial location was examined by taking images every 2 s for 3 min and monitoring the location of the peak concentration. Once the stable band was established, the heat source was translated to 500 μm every 3 min (this is equivalent to a velocity of ~170 μm/min) to generate a quasi-steady moving heat source. As can be seen, the focused band follows the heater image in both directions indicating the successful transport of the focused band from left to right and vice versa. This ability provides the possibility to increase the local concentration of a diluted solution up to a certain level and then transport the concentrated band to, for example, combine with another solution, or to a sensing surface. The optical manipulation of the temperature field would also enable dynamic separation of charged analytes as demonstrated previously with fixed-heater type TGF (Hoebel et al. 2006). This can be done through increasing the local concentration of each analyte by adjusting the light intensity and sequentially separating the focused bands.

4 Conclusions

In this study, an optothermal analyte preconcentration and manipulation method based on temperature gradient focusing (TGF) was introduced for the first time. Optothermal fluid temperature field control was achieved by means of a commercial digital projector; the concentration of a sample analyte, fluorescein, was locally increased; and the focused band was successfully transported along the microchannel by adjusting the image of the heater in an external computer. The proposed method offers the following unique features in its present format:

1. Flexibility-dynamic control of the heater size, location, and power ultimately leads to the dynamic control of the focused band location and its on-demand transportation to the point of analysis, for example, a sensor.
2. Noninvasive heating avoids complex fabrication methods and/or controlling systems as well as predefined focusing geometries.

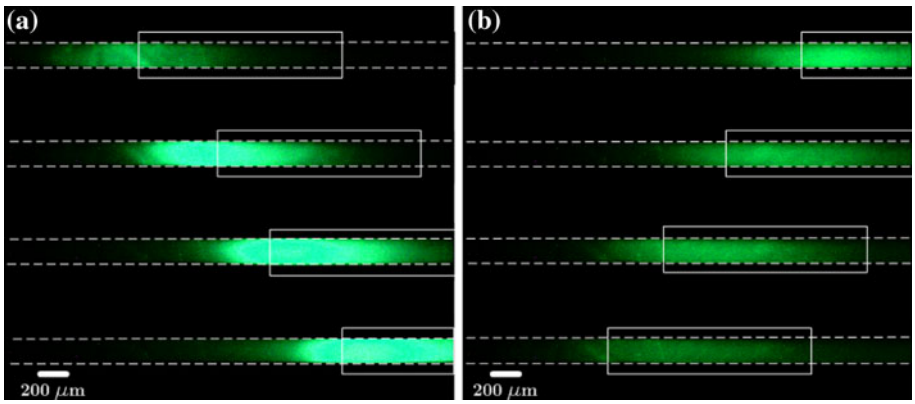

Fig. 7 Image sequence showing the on-demand transport of the focused band of fluorescein by moving the optothermal heater from **a** left to right and **b** right to left. The heater location is indicated by a *white rectangle*. The applied electric field is 200 V/cm with positive polarity on the right and ground on the left reservoirs. A stable focused band was first generated at the start point (the stability was examined by processing a sequence of images taken every 2 s for 3 min) and then transported to the end point by adjusting the heater image. The direction and magnitude of the pressure driven flow was kept constant (pressure was resulting from approximately 25 mm of water hydrostatic head and from right to left) during the experiment. Movies showing the controlled translation of the analyte band are available in Supplementary Material

In addition, the proposed technique enables preconcentration to be performed in short channels, thus smaller footprints may be used. This leads to more compact microdevices and the ability of being integrated with other chemical assays.

Thermal characteristics of the heating system were assessed using a temperature-dependent fluorescent dye. Up to 20°C temperature rise was obtained within 25 s for a heater size of approximately 1.5 mm. The maximum temperature decreases for smaller heater sizes, but the heating rate increases. The preconcentration experiment was performed and up to 500-fold enrichment was obtained within 15 min. Optically controlled transport of the focused band was successfully demonstrated by moving the heater image with a velocity of $\sim$170 μm/min. Future research will include the implementation of the flexibility offered by the proposed technique to separate and translate various analytes sequentially. In addition, a translating heat source could be applied to remove the requirement for pressure-driven flow.

Acknowledgments The authors thank the financial support of the Natural Sciences and Engineering Research Council of Canada NSERC through discovery grants to MB and DS, BC Innovation Council (BCIC) through research scholarship to MA, and the Canada Research Chair Program.

References

Albert M, Debusschere L, Demesmay C, Rocca JL (1997) Large-volume stacking for quantitative analysis of anions in capillary electrophoresis I. Large-volume stacking with polarity switching. J Chromatgr A 757:281–289

Arora A, Simone G, Salieb-Beugelaar GB, Kim JT, Manz A (2010) Latest developments in micro total analysis systems. Anal Chem 82:4830–4847

Astroga-Wells J, Vollmer S, Tryggvason S, Bergman T, Jőrnvall H (2005) Microfluidic electrocapture for separation of peptides. Anal Chem 77:7131–7136

Balss KM, Vreeland WN, Howell PB, Henry AC, Ross D (2004) Micellar affinity gradient focusing: a new method for electrokinetic focusing. J Am Chem Soc 126:1936–1937

Becker M, Mansouri A, Beilein C, Janasek D (2009) Temperature gradient focusing in miniaturized free-flow electrophoresis devices. Electrophoresis 30:4206–4212

Boček P, Deml M, Janák J (1978) Effect of a concentration cascade of the leading electrolyte on the separation capacity in isotachophoresis. J Chromatogr 156:323–326

Burgi DS, Chien R-L (1991) Optimization in sample stacking for high-performance capillary electrophoresis. Anal Chem 63: 2042–2047

Chien R-L, Burgi DS (1992) Sample stacking of an extremely large injection volume in high-performance capillary electrophoresis. Anal Chem 64:1046–1050

Chiou PY, Ohta AT, Wu MC (2005) Massively parallel manipulation of single cells and microparticles using optical images. Nature 436(7049):370–372

Chiou PY, Ohta AT, Jamshidi A, Hsu HY, Wu MC (2008) Light-actuated ac electroosmosis for nanoparticle manipulation. J Microelectromech Syst 17(3):525–531

Duhr S, Braun D (2006) Why molecules move along a temperature gradient. PNAS 103(52):19678–19682

Dupuy A, Lehmann S, Cristol J (2005) Protein biochip systems for the clinical laboratory. Clin Chem Lab Med 43:1219–1302

Erickson D, Sinton D, Li D (2003) Joule heating and heat transfer in poly(dimethylsiloxane) microfluidic systems. Lab Chip 3: 141–149

Everaerts FM, Verheggen PEM, Mikkers FEP (1979) Determination of substances at low concentrations in complex mixtures by isotachophoresis with column coupling. J Chromatogr 169:21–38

Fu R, Xu B, Li D (2006) Study of the temperature field in microchannels of a PDMS chip with embedded local heater using temperature-dependent fluorescent dye. Int J Thermal Sci 45:841–847

Ge Z, Yang C, Tang G (2010) Concentration enhancement of sample solutes in a sudden expansion microchannel with Joule heating. Int J Heat Mass Transfer 53:2722–2731

Grier DG (2003) A revolution in optical manipulation. Nature 424(6950):810–816

Guijt RM, Dodge A, van Dedem GWK, de Rooij NF, Verpoorte E (2003) Chemical and physical processes for integrated temperature control in microfluidic devices. Lab Chip 3:1–4

Hoebel SJ, Balss KM, Jones BJ, Malliaris CD, Munson MS, Vreeland WN, Ross D (2006) Scanning temperature gradient focusing. Anal Chem 78:7186–7190

Huber D, Santiago JG (2007) Taylor–Aris dispersion in temperature gradient focusing. Electrophoresis 28:2333–2344

Isoo K, Terabe S (2003) Analysis of metal ions by sweeping via dynamic complexation and cation-selective exhaustive injection in capillary electrophoresis. Anal Chem 75:6789–6798

Issadore D, Humphry KJ, Brown KA, Sandberg L, Weitz DA, Westervelt RM (2009) Microwave dielectric heating of drops in microfluidic devices. Lab Chip 9:1701–1706

Kaigala GV, Hoang VN, Stickel A, Lauzon J, Manage D, Pilarski LM, Backhouse CJ (2008) An inexpensive and portable microchip-based platform for integrated RT–PCR and capillary electrophoresis. Analyst 133:331–338

Kamande MW, Ross D, Locascio LE, Lowry M, Warner IM (2007) Simultaneous concentration and separation of coumarins using a molecular micelle in micellar affinity gradient focusing. Anal Chem 79:1791–1796

Ke C, Berney H, Mathewson A, Sheeshan MM (2004) Rapid amplification for the detection of *Mycobacterium tuberculosis* using a non-contact heating method in a silicon microreactor based thermal cycler. Sens Actuators B 102(2):308–314

Koegler WS, Ivory CF (1996) Focusing proteins in an electric field gradient. J Chromatgr A 726:229–236

Krishnan M, Erickson D (2011) Creating optically reconfigurable channel based microfluidic systems. IEEE Winter Topicals (WTM) 103–104

Krishnan M, Oark J, Erickson D (2009) Optothermorheological flow manipulation. Optic Lett 34(13):1976–1978

Kumar A, Kwon JS, Williams SJ, Green NG, Yip NK, Wereley ST (2010) Optically modulated electrokinetic manipulation and concentration of colloidal particles near an electrode surface. Langmuir 26(7):5262–5272

Lee DS, Park SH, Yang H, Chung KH, Yoon TH, Kim SJ (2004) Bulk micromachined submicroliter-volume PCR chip with very rapid thermal response and low power consumption. Lab Chip 4:401–407

Liao CS, Lee GB, Wu JJ, Chang CC, Hsieh TM, Huang FC (2005) Micromachined polymerase chain reaction system for multiple DNA amplification of upper respiratory tract infectious diseases. Biosens Bioelectron 20:1341–1348

Liu Y, Rauch CB, Stevens RL, Lenigk R, Yang J, Rhine DB, Grodzinski P (2002) DNA Amplification and hybridization assays in integrated plastic monolithic devices. Anal Chem 74:3063–3070

Liu GL, Kim J, Lu Y, Lee LP (2005) Optofluidic control using photothermal nanoparticles. Nat Mater 5(1):27–32

Matsui T, Franzke J, Manz A, Janasek D (2007) Temperature gradient focusing in a PDMS/glass hybrid microfluidic chip. Electrophoresis 28:4606–4611

Mikkers FEP, Everaerts FM, Verheggen PEM (1979) High-performance zone electrophoresis. J Chromatgr 169:11–20

Munson MS, Danger G, Shackman JG, Ross D (2007) Temperature gradient focusing with field-amplified continuous sample injection for dual-stage analyte enrichment and separation. Anal Chem 79:6201–6207

Myers FB, Lee LP (2009) Innovations in optical microfluidic technologies for point-of-care diagnostics. Lab Chip 8:2015–2031

Oda RP, Strausbauch MA, Huhmer AFR, Borson N, Jurrens SR, Craighead J (1998) Infrared-mediated thermocycling for ultrafast polymerase chain reaction amplification of DNA. Anal Chem 70:4361–4368

Psaltis D, Quake SR, Yang C (2006) Developing optofluidic technology through the fusion of microfluidics and optics. Nature 442(7101):381–386

Quirino JP, Terabe S (1998) Exceeding 5000-fold concentration of dilute analytes in micellar electrokinetic chromatography. Science 282:465–468

Quirino JP, Terabe S (1999) Sweeping of analyte zones in electrokinetic chromatography. Anal Chem 71:1638–1644

Ross D, Johnson TJ, Locascio LE (2001) Temperature measurement in microfluidic systems using a temperature dependent fluorescent dye. Anal Chem 73:2509–2515

Ross D, Locascio LE (2002) Microfluidic temperature gradient focusing. Anal Chem 74:2556–2564

Shackman JG, Ross D (2007) Counter-flow gradient electrofocusing. Electrophoresis 28:556–571

Sommer GJ, Kim SM, Littrel RJ, Hasselbrink EF (2007) Theoretical and numerical analysis of temperature gradient focusing via Joule heating. Lab Chip 7:898–907

Tang G, Yang C (2008) Numerical modeling of Joule heating-induced temperature gradient focusing in microfluidic channels. Electrophoresis 29:1006–1012

Terray A, Oakey J, Marr DWM (2002) Microfluidic control using colloidal devices. Science 296(5574):1841–1844

Tolley HD, Wang Q, LeFebre DA, Lee ML (2002) Equilibrium gradient methods with nonlinear field intensity gradient: a theoretical approach. Anal Chem 74:4456–4463

Toner M, Irimia D (2005) Blood-on-a-chip. Annu Rev Biomed Eng 7:77–103

Vigolo D, Rusconi R, Piazzaa R, Howard A, Stone A (2010) Portable device for temperature control along microchannels. Lab Chip 10:795–798

Wang Q, Tan Y, Gong H (2003) An integrated system for real-time PCR analysis based on microfluidic biochip. Int J Comp Eng Sci 4(2):285–288

Yang H, Choi CA, Chung KH, Jun CH, Kim YT (2004) An independent temperature-controllable microelectrode array. Anal Chem 76(5):1537–1543

Yager P, Edwards T, Fu E, Helton K, Nelson K, Tam MR, Weigl BH (2006) Microfluidic diagnostic technologies for global public health. Nature 442:412–418

Yager P, Domingo GJ, Gerdes J (2008) Diagnostics for global health. Annu Rev Biomed Eng 10:107–144

Yang AHJ, Moore SD, Schmidt BS, Klug M, Lipson M, Erickson D (2009) Optical manipulation of nanoparticles and biomolecules in sub-wavelength slot waveguides. Nature 475(7225):71–75